

This is the accepted manuscript made available via CHORUS. The article has been published as:

Surface-Induced Phase Transformations: Multiple Scale and Mechanics Effects and Morphological Transitions

Valery I. Levitas and Mahdi Javanbakht

Phys. Rev. Lett. **107**, 175701 — Published 19 October 2011

DOI: [10.1103/PhysRevLett.107.175701](https://doi.org/10.1103/PhysRevLett.107.175701)

Surface-Induced Phase Transformations: Multiple Scale and Mechanics Effects and Morphological Transitions

Valery I. Levitas¹ and Mahdi Javanbakht²

¹*Iowa State University, Departments of Aerospace Engineering, Mechanical Engineering, and Material Science and Engineering, Ames, Iowa 50011, USA*

²*Iowa State University, Department of Mechanical Engineering, Ames, Iowa 50011, USA*

Strong, surprising, and multifaceted effects of the width of the external surface layer Δ_ξ and internal stresses on surface-induced pre-transformation and phase transformations (PTs) is revealed. Using our further developed phase-field approach, we found that above some critical Δ_ξ^* , a morphological transition from fully transformed layer to lack of surface pre-transformation occurs for any transformation strain ϵ_t . It corresponds to a sharp transition to the universal (independent of ϵ_t), strongly increasing the master relationship of the critical thermodynamic driving force for PT X_c on Δ_ξ . For large ϵ_t , with increasing Δ_ξ , X_c unexpectedly decreases, oscillates, and then becomes independent of ϵ_t . Oscillations are caused by morphological transitions of fully transformed surface nanostructure. A similar approach can be developed for internal surfaces (grain boundaries) and for various types of PTs and chemical reactions.

Reduction in the total surface energy during PT may lead to various surface-induced phenomena—e.g., surface pre-melting, ordering or disordering, martensitic PT, PT from martensitic variant M_i to variant M_j , and barrierless nucleation [1, 2, 3]. Thus, transformation may start from the surface from *stable* in bulk to *metastable* phases at temperature θ , which may be far from the thermodynamic equilibrium temperature θ_e between phases; namely below θ_e for melting and above θ_e for martensitic PTs. While some of our results are applicable to most of the above PTs, we will focus on PTs during cooling, which include martensitic PTs. When the thermal driving force $X = (1 - \theta/\theta_e)/(1 - \theta_c/\theta_e)$ (θ_c is the temperature of the loss of stability of the parent phase) for martensitic PT increases and approaches zero, a few nanometers thick transformed layer appears, grows, and loses its thermodynamic stability, and transformation propagates through the entire sample. Phase-field or Ginzburg-Landau (GL) approach is widely used for simulation of the surface-induced PTs [3, 4, 5, 6]. PT in this approach is described in terms of evolution of a single or multiple order parameter(s). The martensitic

PT below is described by n order parameters η_i that vary from 0 for austenite **A** to 1 for martensitic variant **M_i**. Melting is described by the same potential for a single order parameter [6]. Significant advances were recently achieved in generalization for multivariant martensitic PTs, formulation of a noncontradictory expression for surface energy versus η_i , coupling to advanced mechanics, and consistent expression for interface tension [5, 6].

Despite this progress, two major contradictions are present in the current GL approaches to surface-induced phenomena. (a) While GL approach resolves finite width Δ_η of interfaces that are responsible for PTs, external surface is sharp, although its width is comparable to Δ_η . (b) A sharp external surface also does not permit a correct introduction of surface tension using the method that we developed for the phase interfaces [5, 6]. The goal of this paper is to introduce and study the effect of finite-width of an external surface coupled to mechanics with the help of our further developed GL approach. Thus, a surface (e.g., solid-gas) layer of the width Δ_ξ is described by a solution of GL equation for an additional order parameter ξ . Obtained results (Figs. 1-6) revealed multiple unexpected effects of the surface layer and mechanics, including morphological transitions in the nanostructure, which drastically change our understanding and interpretation of transformation behavior and results of measurements. Deformation of crystal lattice of **A** into lattice of **M_i** is described by transformation strain tensor ϵ_{ti} , which in our case is taken for cubic-tetragonal PT in NiAl. To elucidate the effect of internal stress generated by ϵ_{ti} in different materials, we considered transformation strain $k\epsilon_{ti}$ with $0 \leq k \leq 1$. With increasing X , a stationary nanostructure $\eta_i(\mathbf{r})$ (\mathbf{r} is the position vector) varies (Fig. 4). The critical surface nanostructure $\eta_c(\mathbf{r})$ corresponds to the critical driving force X_c above which the entire sample transforms.

For neglected mechanics, two branches on the curve X_c versus dimensionless width of the surface layer $\overline{\Delta_\xi} = \Delta_\xi/\Delta_\eta$ are obtained (Fig. 1b). For $\overline{\Delta_\xi} \ll 1$, the effect of the surface layer is negligible and X_c and η_c are the same as for the sharp surface. However, for some critical and quite small $\overline{\Delta_\xi}^* = 0.166$, the slope of the curve $X_c(\overline{\Delta_\xi})$ has an unexpected jump and a drastic increase in the critical driving force occurs with increasing $\overline{\Delta_\xi}$. Critical nanostructure undergoes morphological transition at this point, from a homogeneous layer along the surface with the maximum value $\eta_c^{max} \simeq 1$ (as in Figs. 2a-b), to a thin strip in the middle of the surface layer with very small $\eta_c^{max} \simeq 10^{-5}$. This means that as soon as barrierless nucleation

starts from the surface, it spreads over the entire sample. Allowing for mechanics (i.e., energy of internal stresses) increases X_c with increasing magnitude of the transformation strain k , as expected. However, for some critical width $\overline{\Delta}_\xi^*(k)$, the curve $X_c(\overline{\Delta}_\xi, k)$ for any k reaches the master curve for neglected mechanics $X_c^0(\overline{\Delta}_\xi)$ ($k = 0$) and coincides with it for larger $\overline{\Delta}_\xi$. A jump in slope in all curves $X_c(\overline{\Delta}_\xi, k)$ at $\overline{\Delta}_\xi^*(k)$ is accompanied by a morphological transition to very small $\eta_c^{max} \simeq 10^{-5}$, as with neglected mechanics. This transition explains the lack of the effect of elastic energy on the critical driving force for PT X_c for $\overline{\Delta}_\xi > \overline{\Delta}_\xi^*(k)$: because for the critical nanostructure η_c^{max} is very small, then the transformation strain and elastic energy are negligible as well. While for $k = 1/3$ the critical driving force for PT is practically independent of $\overline{\Delta}_\xi < \overline{\Delta}_\xi^*$ (as with neglected mechanics), for $k = 2/3$ and 1, X_c surprisingly reduces with increasing $\overline{\Delta}_\xi$ before morphological transition and the curve $X_c(\overline{\Delta}_\xi, k)$ has a ν -shape at the morphological transition point $\overline{\Delta}_\xi^*(k)$. One more finding is that for $k = 1$, there is oscillation at the curve $X_c(\overline{\Delta}_\xi)$ caused by three morphological transitions in the critical nanostructure (Fig. 2). We designate contractions of tensors over one and two indices as $\mathbf{A} \cdot \mathbf{B} = \{A_{ij} B_{jk}\}$ and $\mathbf{A} : \mathbf{B} = A_{ij} B_{ji}$, respectively; ∇ is the gradient operator in the deformed state.

Phase-field model. The current model generalizes our recently developed model [5] by including the surface layer. Thus, an additional order parameter ξ describes a smooth transition between solid ($\xi = 0$) and surrounding ($\xi = 1$), e.g., gas. The full model is presented in supplementary materials [7]. Here, we will discuss the structure of new equations only. The Helmholtz free energy per unit undeformed volume,

$$\begin{aligned} \psi &= \psi^e + \frac{\rho_0}{\rho} \check{\psi}^\theta + \psi^\theta + \frac{\rho_0}{\rho} \psi^\nabla + \frac{\rho_0}{\rho} \psi_\xi(\xi, \nabla \xi, \eta_k); \\ \psi^e &= 0.5(1 - \phi(\xi))(K\varepsilon_{0e}^2 + 2\mu \mathbf{e}_e : \mathbf{e}_e); \phi(\xi) = \xi^2(3 - 2\xi), \end{aligned} \quad (1)$$

contains the energy $\psi_\xi(\xi, \nabla \xi, \eta_k)$ for surface layer and the elastic energy ψ^e with bulk K and shear μ moduli, which smoothly reduce to zero within surface layer. Here, $\frac{\rho_0}{\rho}$ are the ratio of mass densities in the undeformed and deformed states, $\check{\psi}^\theta$, ψ^θ , and ψ^∇ are the contributions to ψ related to the double-well barrier, thermal energy, and energy related to $\nabla \eta_i$, ε_{0e} and \mathbf{e}_e are the elastic volumetric and deviatoric strains. The energy of the surface layer per unit deformed volume is [7]

$$\psi_\xi = J\xi^2(1 - \xi)^2 + 0.5\beta_\xi(\nabla \xi)^2 =$$

$$q(\eta_i)/\Delta_\xi \left(16.62\xi^2(1-\xi)^2 + 0.542\Delta_\xi^2(\nabla\xi)^2 \right), \quad (2)$$

where β_ξ and J are the parameters, and $q(\eta_i)$ is the surface energy of the sharp external surface. Eqs.(1) and (2) lead to the GL equations for ξ and η_i :

$$\begin{aligned} \frac{1}{L_\xi} \frac{\partial \xi}{\partial t} &= \frac{q(\eta_i)}{\Delta_\xi} \left(1.083\Delta_\xi^2 \nabla^2 \xi - 66.48\xi(1-\xi)(0.5-\xi) \right) \\ &\quad - \frac{\rho}{\rho_0} \frac{\partial \psi^e}{\partial \xi}; \end{aligned} \quad (3)$$

$$\frac{1}{L} \frac{\partial \eta_i}{\partial t} = -\frac{\rho}{\rho_0} \frac{\partial \psi}{\partial \eta_i} \Big|_\epsilon + \nabla \cdot \left(\frac{\rho}{\rho_0} \frac{\partial \psi}{\partial \nabla \eta_i} \right), \quad (4)$$

where L and $L_\xi \gg L$ are the kinetic coefficients. For neglected ψ^e , Eq.(3) has solution for a stationary surface layer [6]: $\xi_s = [1 + \exp(5.54x/\Delta_\xi)]^{-1}$. For neglected mechanics and single stationary surface layer orthogonal to x , Eq.(3) simplifies to ($\bar{\psi}^\theta = \check{\psi}^\theta + \psi^\theta$)

$$\frac{1}{L} \frac{\partial \eta_i}{\partial t} = \beta \nabla^2 \eta_i - \frac{\partial \bar{\psi}^\theta}{\partial \eta_i} - \frac{33.24}{\Delta_\xi} \frac{\partial q(\eta_i)}{\partial \eta_i} \xi_s^2 (1 - \xi_s)^2. \quad (5)$$

Problem formulation. Material parameters, initial and boundary conditions are given in [7]. The finite element code COMSOL was utilized for plane stress 2D problems. Rectangular $25 \times 12.5 \text{ nm}^2$ sample discretized with triangle Lagrange elements with quadratic approximation was treated. All sides are stress-free, excluding zero vertical displacement at the upper and lower horizontal sides. Surface layer was introduced at the right vertical line only. We considered: GL equation without mechanics; GL equations with mechanics, for $k = 1/3, 2/3, 1$, with elastic properties independent of ξ and without surface stresses; the same with elastic properties dependent on ξ ; and the same with surface stresses. *Scale effects and morphological transitions.* First, the simplest model (Eq.(5)) with neglected mechanics (which is generic for various types of PTs) is analyzed. Since the magnitude of the local contribution of the surface layer to the GL Eq.(5) scales with $1/\Delta_\xi$ (Fig. 1a), an increase in Δ_ξ should suppress nucleation. Also, for $\overline{\Delta_\xi} \ll 1$ the results should coincide with those for the sharp external surface. Both of these predictions are confirmed by numerical simulations (Fig. 1b); however, all other results are counterintuitive and unexpected. The critical thermodynamic driving force for PT X_c vs. $\overline{\Delta_\xi}$ and some corresponding critical nanostructures for single \mathbf{M}_1 are presented in Figs. 1-2, respectively. For neglected mechanics, the numerical solution for $\xi(x)$ is well described

by $\xi_s(x)$; thus simple Eq.(5) is valid. Two branches on the curve $X_c(\overline{\Delta_\xi})$ are obtained (Fig. 1b). For $\overline{\Delta_\xi} \ll 1$, the effect of the surface layer is negligible; X_c , η_c , and interface velocity for $X > X_c$ are practically the same as for the sharp surface; stationary and nonstationary solutions are independent of y , $\eta_c^{max} = 1$, and width of the transformed surface layer δ_{sl} (determined from $\eta_c = 0.5$) is essentially larger than Δ_ξ (Fig. 3; plots in Figs. 3-5 are for the middle line of the sample). However, above some critical and quite small $\overline{\Delta_\xi}^* = 0.166$, an unexpected jump to a completely different regime occurs. Critical nanostructure undergoes morphological transition to a thin strip in the middle of the surface layer with very small $\eta_c^{max} \simeq 10^{-5}$. Consequently, as soon as surface barrierless nucleation starts, PT spreads over the entire sample; thus, pre-transformation does not exist. The slope of the curve $X_c(\overline{\Delta_\xi})$ has a jump (explained by a morphological transition), and a drastic increase in the critical driving force occurs with increasing $\overline{\Delta_\xi}$. For coupled GL and mechanics formulation (yet with neglected surface stresses and change in elastic properties), X_c increases with increasing magnitude of the transformation strain k . This is expected because of suppressing contribution of the energy of internal stresses. For critical nanostructure, while it is homogeneous along y , the width of the transformed layer δ_{sl} decreases with increasing k (Fig. 3) and η_c^{max} is becoming smaller than 1. However, for some critical width $\overline{\Delta_\xi}^*(k)$, the curve $X_c(\overline{\Delta_\xi}, k)$ for any k reaches the curve $X_c^0(\overline{\Delta_\xi})$ for $k = 0$ and coincides with it for larger $\overline{\Delta_\xi}$ (Fig. 1b). That is why we call $X_c^0(\overline{\Delta_\xi})$ the universal (i.e., independent of ϵ_t and internal stresses) master dependence. At $\overline{\Delta_\xi}^*(k)$ a jump in slope in all curves $X_c(\overline{\Delta_\xi}, k)$ occurs, which is caused by morphological transition to very small $\eta_c^{max} \simeq 10^{-5}$, similar to the case with neglected mechanics. This transition explains coincidence of the curves for different k , i.e., the lack of the effect of elastic energy on X_c for $\overline{\Delta_\xi} > \overline{\Delta_\xi}^*(k)$. Indeed, since for critical nanostructure η_c^{max} is very small, then ϵ_t and elastic energy are negligible as well. This result leads to new intuition for such a complex nonlinear interaction between PT, surface phenomena, and mechanics.

While for $k = 1/3$ X_c does not change with increasing width of the surface layer (like for neglected mechanics), for $k = 2/3$ and 1, X_c surprisingly reduces with increasing $\overline{\Delta_\xi} < \overline{\Delta_\xi}^*$ and the curve $X_c(\overline{\Delta_\xi})$ has a ν -shape at the morphological transition point $\overline{\Delta_\xi}^*(k)$ (Fig. 1b). For $k = 1$, there is also oscillation at the curve $X_c(\overline{\Delta_\xi})$, caused by three morphological transitions of the critical nanostructure (Fig. 2). Thus, almost homogeneous along y nanostructure for

the sharp surface and $\overline{\Delta}_\xi = 0.066$ changes to three different types of localized structures. Such a structure is a result of competition between a promoting effect of the surface layer and a suppressing effect of elastic stresses; localized structure leads to a reduction in elastic energy. When variable elastic properties are included for $k = 1$, results for small $\overline{\Delta}_\xi$ are similar to that with constant properties, i.e., there are some oscillations in $X_c(\overline{\Delta}_\xi)$. However, reduction in X_c with growing $\overline{\Delta}_\xi$ is much smaller, critical $\overline{\Delta}_\xi^*$ for morphological transition to small η_c^{max} is larger, and critical nanostructure is independent of y without morphological transitions below $\overline{\Delta}_\xi^*$. For the complete model, when in addition the interface and surface tensions [7] are taken into account, X_c increases for all $\overline{\Delta}_\xi$ because of suppressing effect of additional compression stresses on transformational expansion along the surface. Pre-transformation starts at X significantly smaller than X_c (especially for small $\overline{\Delta}_\xi$) but $\eta(\mathbf{r})$ did not change substantially, while X increases up to X_c (Fig. 4). Such low sensitivity of surface nanostructure to the driving force, within some range, may have practical importance. Critical nanostructure is independent of y up to $\overline{\Delta}_\xi < 0.664$, above which it advances more at the sample center.

Examples of evolution of nanostructure for single and two martensitic variants after critical nanostructure loses its stability after a slight increase in X are given in Figs. 5-6 and supplementary movies [7]. The case with two variants is much more complicated for analysis due to the possibility of reduction of elastic energy by combining variants and additional scale parameters (the width of M_1 - M_2 interface). To summarize, very strong and multifaceted effects of the width of the external surface layer Δ_ξ and internal stresses on surface-induced pre-transformation and PT was revealed using our extended phase-field approach. Obtained results change our understanding of surface-induced PTs and interpretation of experimental data. For neglected mechanics (which is an acceptable approximation for melting, amorphization, and for small transformation strain components along the surface), thermodynamic conditions for the possibility of surface-induced PT are [2, 3] $\Gamma = \gamma_M - \gamma_A + E_\eta < 0$, where γ is the surface energy. Our results show that for the chosen material parameters it is true for quite small $\Delta_\eta \geq 6\Delta_\xi$ only. The fact that surface-induced melting was observed for various materials [2, 3] means that solid-liquid interface is much thicker than solid-gas interface. For a thinner phase interface, stationary surface-molten layer cannot exist and surface-induced PT occurs spontaneously in the entire sample after some overheating. Lack of surface-molten layer and

necessity for overheating was observed for various materials and specific orientations [2, 3] and was usually interpreted as a consequence of $\Gamma > 0$. It is known [2, 3] that due to a significant error in determining each of three surface energies in the above criterion, it is difficult to predict a priori whether surface melting will occur. The same is valid for other PTs, such as martensitic PTs and amorphization [1]. Our results show that surface-induced transformation should not necessarily occur at $\Gamma < 0$ and that $\overline{\Delta_\xi}$ is an additional key parameter that strongly affects surface-induced transformation and X_c . While allowing for finite $\overline{\Delta_\xi}$ suppresses surface-induced PT for zero or small transformation strain, for larger ϵ_t there is a range of $\overline{\Delta_\xi}$ for which an increase in $\overline{\Delta_\xi}$ promotes PT; however, for larger $\overline{\Delta_\xi}$, PT is again suppressed. Finding ways to control Δ_ξ (e.g., by changing the composition or the surrounding of the surface layer) will allow one to control the surface-induced phenomena and nanostructures. E.g., $\beta - \delta$ PT at the surface of the β occurs at θ_e in the presence of nitroplastiziers only [8]. The revealed low sensitivity of surface nanostructure to the driving force, within some range, also may have practical importance. A similar approach can be developed for internal surfaces (grain boundaries and immobile interfaces inside of composite or multiphase materials) and for various types of PTs (electromagnetic, diffusive-displacive, and amorphization) and chemical reactions. Melting and amorphization at grain boundaries for various materials [1] are corresponding examples. The support of NSF, ARO, DTRA, AFOSR, and ISU is gratefully acknowledged.

FIGURE CAPTIONS

FIG. 1 (color online). (a) Plot of the ξ -dependent term $\xi_s^2(1 - \xi_s)^2/\Delta_\xi$ in GL Eq.(5) vs. $\bar{x} = x/\Delta_\eta$ for different Δ_ξ . (b) Critical thermodynamic driving force X_c vs. $\overline{\Delta_\xi}$ for a single M_1 and different cases: neglected mechanics (GL), coupled GL and mechanics with transformation strain of $\epsilon_t/3$, $2\epsilon_t/3$, and ϵ_t as well as with variable elastic properties $(\epsilon_t, \phi(\xi))$, and interface σ_η^{st} and surface σ_ξ^{st} tensions $(\epsilon_t, \phi(\xi), \sigma^{st})$. The curve X_c^0 is approximated as $X_c^0 = 1 - 0.267\overline{\Delta_\xi}^{-2/3}$.

FIG. 2 (color online). Critical nanostructures for the coupled GL and mechanics with ϵ_t for a single M_1 and some values of dimensionless width of the surface layer $\overline{\Delta_\xi}$. Three morphological transitions are observed with increasing $\overline{\Delta_\xi}$.

FIG. 3 (color online). Profiles of the single order parameter η for $\overline{\Delta_\xi} = 0$ and the order parameters η and ξ for $\overline{\Delta_\xi} = 0.066$ for different cases (described in Fig. 1b) vs. \bar{x} .

FIG. 4 (color online). Profiles of the single order parameter η vs. \bar{x} for some values of $\overline{\Delta_\xi}$ for critical nanostructures (solid line) and nanostructures for smaller thermodynamic driving forces (dashed line) for the $(\epsilon_t, \phi(\xi), \sigma^{st})$ model.

FIG. 5 (color online). Evolution of surface nanostructure for $X > X_c$ and two different values of $\overline{\Delta_\xi}$ for the case with transformation strain of ϵ_t and a single martensitic variant.

FIG. 6 (color online). Evolution of surface nanostructure for two martensitic variants for different values of $\overline{\Delta_\xi}$ and the same thermodynamic driving force $X = 0.7915$.

References

- [1] J. Luo and Y. Chiang, *Annu. Rev. Mater. Res.* **38**, 227-49 (2008); S. Li *et al.*, *Phys. Rev. B* **81**, 245433 (2010); M. I. Haftel and K. Gall, *Phys. Rev. B* **74**, 035420 (2006); J. O. Indekeu, *Physica A* **389**, 4332 (2010).
- [2] A. W. Denier van der Gon *et al.*, *Surf. Sci.* **227**, 143 (1990); Q. S. Mei and K. Lu, *Prog. Mater. Sci.* **52**, 1175 (2007).
- [3] R. Lipowsky, *Phys. Rev. Lett.* **49**, 1575 (1982); B. Pluis, D. Frenkel and J. Van der Veen, *Surf. Sci.* **239**, 282 (1990).
- [4] V. I. Levitas, D.-W. Lee, and D. L. Preston, *Europhys. Lett.* **76**, 81 (2006).
- [5] V. I. Levitas and M. Javanbakht, *Phys. Rev. Lett.* **105**, 165701 (2010).
- [6] V. I. Levitas and K. Samani, *Nat. Commun.* **2**, 284 (2011).
- [7] Supplementary Material, <http://link.aps.org/supplemental/xxx>.
- [8] V. I. Levitas *et al.*, *J. Appl. Phys.* **102**, 113502 (2007).

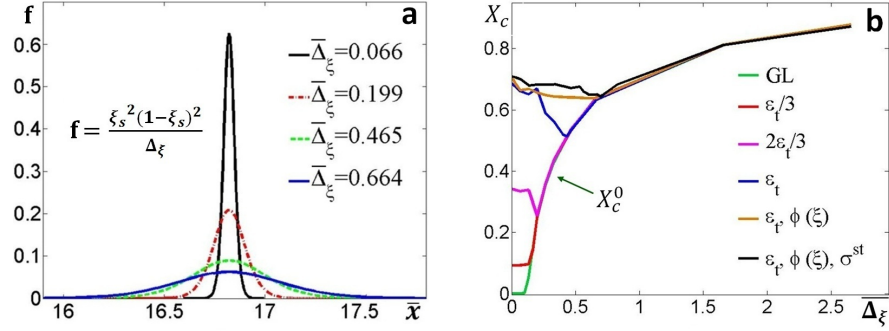


FIG. 1 (color online). (a) Plot of the ξ -dependent term $\xi_s^2(1-\xi_s)^2/\Delta_\xi$ in GL Eq.(5) vs. $\bar{x} = x/\Delta_\eta$ for different Δ_ξ . (b) Critical thermodynamic driving force X_c vs. Δ_ξ for a single M_1 and different cases: neglected mechanics (GL), coupled GL and mechanics with transformation strain of $\epsilon_t/3$, $2\epsilon_t/3$, and ϵ_t as well as with variable elastic properties ($\epsilon_t, \phi(\xi)$), and interface σ_η^{st} and surface σ_ξ^{st} tensions ($\epsilon_t, \phi(\xi), \sigma^{st}$). The curve X_c^0 is approximated as $X_c^0 = 1 - 0.267\bar{\Delta}_\xi^{-2/3}$.

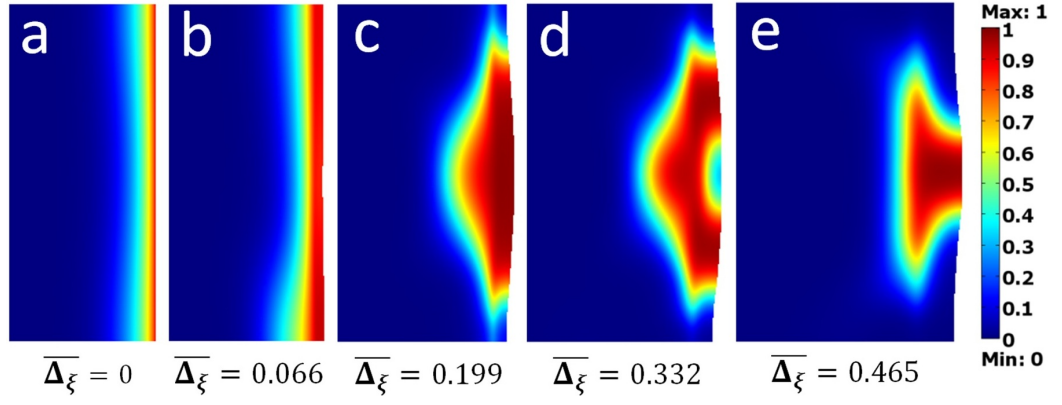


FIG. 2 (color online). Critical nanostructures for the coupled GL and mechanics with ϵ_t for a single M_1 and some values of dimensionless width of the surface layer $\overline{\Delta}_\xi$. Three morphological transitions are observed with increasing $\overline{\Delta}_\xi$.

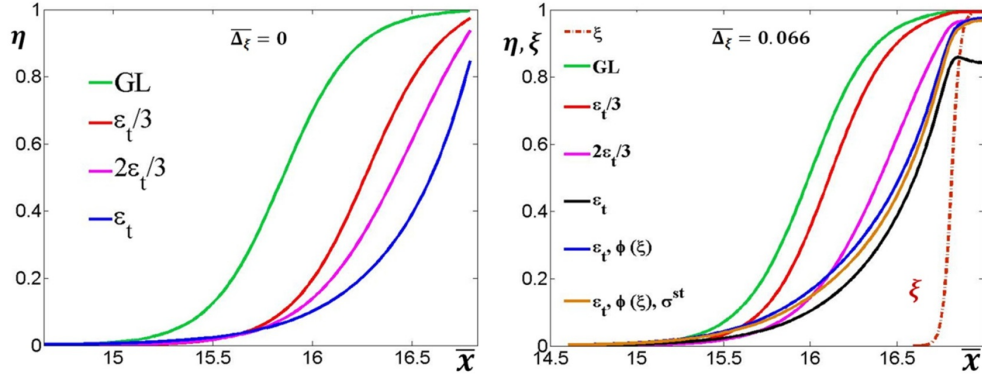


FIG. 3 (color online). Profiles of the single order parameter η for $\bar{\Delta}_\xi = 0$ and the order parameters η and ξ for $\bar{\Delta}_\xi = 0.066$ for different cases (described in Fig. 1b) vs. \bar{x} .

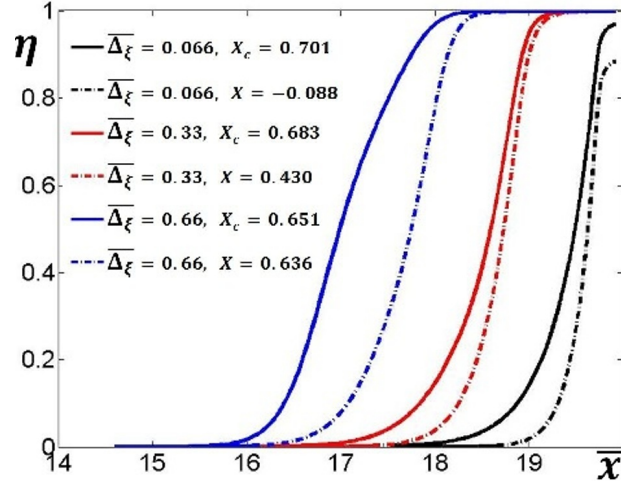


FIG. 4 (color online). Profiles of the single order parameter η vs. \bar{x} for some values of $\overline{\Delta}_\xi$ for critical nanostructures (solid line) and nanostructures for smaller thermodynamic driving forces (dashed line) for the $(\epsilon_t, \phi(\xi), \sigma^{st})$ model.

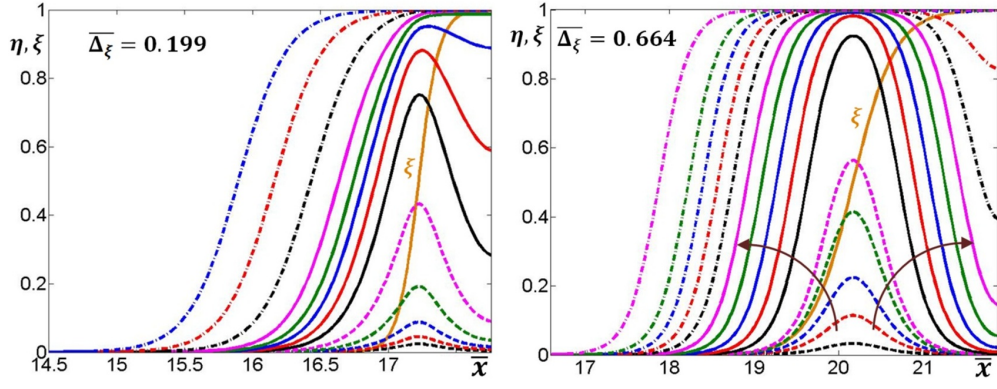


FIG. 5 (color online). Evolution of surface nanostructure for $X > X_c$ and two different values of $\overline{\Delta_\xi}$ for the case with transformation strain of ϵ_t and a single martensitic variant.

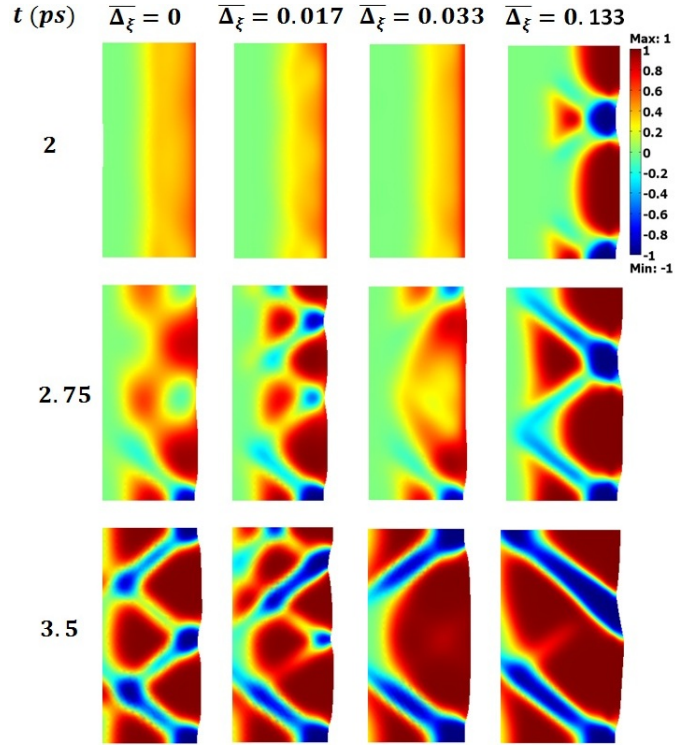


FIG. 6 (color online). Evolution of surface nanostructure for two martensitic variants for different values of $\overline{\Delta\xi}$ and the same thermodynamic driving force $X = 0.7915$.